

Coordinate depression of bradykinin receptor recycling and microtubule-dependent transport by taxol

SARAH F. HAMM-ALVAREZ*[†], BRUCE E. ALAYOF[‡], HERBERT M. HIMMEL[‡], PRESTON Y. KIM*, ANNE L. CREWS[‡], HAROLD C. STRAUSS[‡], AND MICHAEL P. SHEETZ*[§]

Departments of *Cell Biology and of [‡]Medicine and Pharmacology, Duke University Medical Center, Durham, NC 27710

Communicated by Thomas S. Reese, March 15, 1994

ABSTRACT Significant cardiovascular side effects have limited the use of taxol as an anticancer drug. A link between decreased plasma membrane dynamics and taxol has been implied because taxol can inhibit intracellular vesicle movements. Reduced membrane recycling caused by taxol could inhibit agonist-evoked Ca^{2+} signaling within endothelial cells, resulting in endothelium-dependent vasodilation. Bradykinin and ATP are two agonists that evoke Ca^{2+} transients in endothelial cells. Since the bradykinin receptor-agonist complex is internalized and recycled whereas the ATP agonist-receptor complex is not, we expected that a taxol inhibition of recycling would decrease bradykinin but not ATP receptor activity. We found that taxol depresses (i) the frequency (to 41% of control) and velocity (to 55% of control) of microtubule-dependent vesicle transport and (ii) bradykinin-evoked cytosolic Ca^{2+} transients (to 76% of control) in bovine aortic endothelial cells. In studying bradykinin receptor desensitization, which reflects receptor recycling, we demonstrate that taxol inhibits bradykinin-evoked Ca^{2+} transients by 50%. Taxol did not significantly alter ATP-evoked Ca^{2+} transients in either single-exposure or desensitization experiments. We suggest that taxol's reduction of bradykinin-evoked Ca^{2+} transients is due to altered microtubule-dependent membrane recycling. This report describes taxol's ability to alter plasma membrane composition through effects on vesicle transport and membrane trafficking pathways. This finding provides a possible mechanism by which taxol can substantially alter cardiovascular function.

Taxol, originally isolated from the bark of a western yew, *Taxus brevifolia*, was initially found to be highly cytotoxic against several murine tumors (1), and it now appears to be effective against many different tumor types (2). Taxol is one of several cell cycle-targeted chemotherapeutics including vincristine and vinblastine that inhibit mitosis by interference with the microtubule (MT) mitotic spindle. Since taxol inhibits mitosis by MT stabilization (3), it is distinct from the other MT-targeted chemotherapeutics that inhibit mitosis by MT destabilization.

Despite its success in treatment of a variety of solid tumors including ovarian, breast, and lung, assessment of taxol toxicity in clinical trials has revealed a disturbingly high (30–40%) incidence of cardiac bradyarrhythmias and tachyarrhythmias and, in a small number of patients, the more serious complications of myocardial ischemia and infarction (2). These latter episodes of myocardial ischemia and infarction suggest that an understanding of the cardiovascular effects of taxol may be of importance. Since cell cycle chemotherapeutics usually exhibit their principal side effects in rapidly dividing cells, these reported incidences of cardiovascular toxicity are puzzling and also unique to taxol relative to other MT-targeted chemotherapeutics.

In interphase cells in culture, MTs are often organized in a radial array around a single MT-organizing center (MTOC) located near the nucleus and the Golgi apparatus. Increasing evidence has implicated MT-dependent vesicle transport along interphase MTs in cellular membrane trafficking (4, 5). Taxol causes a major reorganization of MTs within cells by catalyzing the assembly of MTs from sites other than the MTOC (3, 6). We have recently reported that taxol, like nocodazole, inhibits MT-dependent vesicle transport in CV-1 cells (6). It is logical, then, to postulate that taxol might alter endocytic processing and receptor recycling, processes that involve MT-dependent vesicle transport.

Taxol's cardiovascular toxicity could be linked to an alteration in density of plasma membrane receptors caused by disruption of MT-dependent transport. Receptors that might be critically important in the development of cardiovascular toxicity would be those coupled to Ca^{2+} -signaling pathways. We have evaluated the effects of taxol on two such receptors, the bradykinin (BK) receptor and the ATP receptor, which undergo different degrees of desensitization during agonist exposure, apparently because of their distinct recycling pathways. Recent studies have shown that BK binding is followed by internalization of the BK-BK receptor complex, release of BK in the endosomal pathway, and recycling of the BK receptor from the late endosomes or trans-Golgi network (7, 8). In contrast, all available evidence indicates that ATP binding to its receptor does not promote receptor internalization and/or recycling or degradation (7). These two receptors constitute distinct models for determination of the effects of taxol on receptor recycling. If taxol alters receptor recycling, then functional differences in the agonist-evoked responses between plasmalemmal BK receptors and ATP receptors should be detectable.

We have examined taxol's effects on MT-dependent vesicle movements, cellular organization, and plasma membrane composition in bovine aortic endothelial cells (BAECs). We found that taxol significantly inhibits the frequency and velocity of small MT-dependent vesicle movements in these cells. Both MT and Golgi organization were altered by taxol. When agonist (BK or ATP)-evoked Ca^{2+} transients were measured, we found that taxol inhibited BK but not ATP effects. Our results suggest that taxol alters the plasma membrane density of the BK receptor, but not the ATP receptor. This is consistent with our view that taxol can affect plasma membrane composition by altering MT-dependent membrane trafficking pathways.

Abbreviations: MT, microtubule; MTOC, microtubule-organizing center; BK, bradykinin; BAEC, bovine aortic endothelial cell; DIC, differential interference contrast; VSV-G, vesicular stomatitis virus G glycoprotein; $[Ca^{2+}]_i$, intracellular calcium concentration.

[†]Present address: Department of Pharmaceutical Sciences, University of Southern California School of Pharmacy, 1985 Zonal Avenue, Los Angeles, CA 90033.

[§]To whom reprint requests should be addressed.

The publication costs of this article were defrayed in part by page charge payment. This article must therefore be hereby marked "advertisement" in accordance with 18 U.S.C. §1734 solely to indicate this fact.

MATERIALS AND METHODS

Materials. Taxol was purchased from Calbiochem. Monoclonal antibody YOL1/34 was obtained from Accurate Chemicals. Antibody P5D4 was obtained from Thomas Kreis (University of Geneva, Switzerland). EM grade glutaraldehyde and paraformaldehyde were obtained from Polyscience. Brij 35 and Triton X-100 were obtained from Pierce. Fetal bovine serum was obtained from HyClone. All other media and additives used in tissue culture were obtained from GIBCO/BRL. The acetoxymethyl ester of fura-2 (fura-2 AM) was from Molecular Probes. All other biochemicals were purchased from Sigma.

Cell Culture and Treatment of BAECs. Endothelial cells were collected from bovine aortas as described (9) and cultured in DMEM containing 10% fetal calf serum and 1× antibiotic/antimycotic solution. Greater than 95% of the cells prepared in this way stained for factor VIII antigen and express angiotensin-converting enzyme activity. Cultures were split 1:4 for subculture at confluence (3–5 days) with 0.05% trypsin/0.53 mM EDTA. Only cells between the second and eighth passage were used.

For video microscopy, BAECs were plated at low density on sterile 20 × 40 mm no. 1 glass coverslips. Exposure to taxol or vehicle was in a Petri dish for 60 min at 37°C in conditioned medium. For nocodazole treatment, MTs were depolymerized by incubation of the cells on ice for 30 min, followed by exposure of the cells to nocodazole at 1 µg/ml on ice for 20 min, and recovery at 37°C for 30 min prior to observation of vesicle movements. To infect BAECs with ts045 (the temperature-sensitive mutant of the virus encoding VSV-G), cells on coverslips were exposed to a high titer stock of ts045 and incubated at 32°C for 1 hr. After extensive rinsing with PBS, fresh medium was added, and the cells were incubated for 3 hr at 39°C. The cells were then incubated at 32°C for selected times prior to fixation.

Immunofluorescence Studies. Visualization of samples was with a Zeiss Axiophot (×100 Neofluar objective) equipped with a Photometrics Star 1 charge-coupled device camera. Extraction and fixation of MTs was as described (6). For visualization of vesicular stomatitis virus G glycoprotein (VSV-G) by immunofluorescence, BAECs were fixed, stained, and mounted as described (10) using the P5D4 primary antibody to the VSV-G (11).

Video-Enhanced Differential Interference Contrast (DIC) Microscopy and Analysis. A Zeiss inverted microscope equipped with fiber-optic illumination and a ×100/1.3 numerical aperture objective was attached to a Dage-MTI VE-1000 camera (newvicon tube) and a Hamamatsu/Argus 10 image processor and used for video-enhanced DIC microscopy as described (12). Data were recorded on s-VHS tapes. An air curtain incubator maintained the microscope stage at 37°C.

Analysis of the frequency and run length of vesicle movements in BAECs within a defined area of each cell was as described (6). Only vesicles ≤300 nm in diameter that moved for distances ≥1 µm were included. Control and treated BAECs (10 cells per plate) were observed, and differences in vesicle movements were evaluated for statistical significance at the $P \leq 0.05$ level by using a *t* test.

Measurement of the Intracellular Calcium Concentration ($[Ca^{2+}]_i$) elicited by BK and ATP. Fluorescence was quantitated using a Deltascan system (Photon Technology International, Princeton, NJ) coupled to an inverted epifluorescence microscope (Nikon Diaphot) and a single beam photomultiplier tube (Hamamatsu, Middlesex, NJ). Single cells were alternately excited at 340 and 380 nm, and emitted light was collected by a photomultiplier tube (510 ± 10 nm). Photon sampling was restricted to the target area, and fluorescence

emission at the two excitation wavelengths was stored for subsequent analysis.

BAECs were plated at very low density on glass coverslips and loaded with fura-2 AM at 1 µM for 30 min. Taxol-treated cells were incubated with 4 µM taxol for 60 min prior to fura-2 AM loading. Coverslips with the fura-2-loaded BAECs were transferred to the epifluorescence microscope, where a cell was randomly selected for study. The experimental chamber was perfused with HEPES-buffered physiological salt solution at a rate of 0.5 ml/min at room temperature.

RESULTS

Small Vesicle Movements in BAECs Are MT-Dependent and Inhibited by Taxol. Subconfluent BAECs on glass coverslips assume a fibroblast-type morphology. The peripheral regions of these cells are <1 µm thick and ideal for imaging of small vesicle movements with video-enhanced DIC microscopy. Fig. 1 shows images of control and taxol-treated BAECs as seen by video-enhanced DIC microscopy with representative vesicles (≤300 nm in diameter) marked by arrows. After treatment with the MT poison, nocodazole (1 µg/ml), the frequency of small vesicle movements in BAECs is reversibly reduced to $1\% \pm 2\%$ of the levels seen in control cells ($n = 10$), suggesting that the small vesicles that we observe in our assay are moving along MTs. The frequency of small vesicle movements of this same vesicle population in BAECs is significantly ($P \leq 0.05$) inhibitable by taxol. Taxol (4 µM, 60 min) reduced the frequency of MT-dependent vesicle movements to $41\% \pm 7\%$ of that seen in controls. Incubation in taxol-free media for 60 min at 37°C reversed this effect.

A dose-response curve for inhibition of the frequency of MT-dependent vesicle movements in BAECs by taxol is shown in Fig. 2, from which an IC_{50} value was calculated to be 1 µM. Inhibition of vesicle movements became significant ($P \leq 0.05$) at doses of taxol ≥500 nM. Taxol also significantly ($P \leq 0.05$) reduced the velocity of vesicle transport (Table 1) at concentrations ≥200 nM.

Taxol Alters MT Organization in BAECs. In BAECs grown to subconfluency on glass, MTs form a radial array around a single MTOC, with the (–) ends clustered in the perinuclear region at the MTOC near the Golgi apparatus, and the (+) ends radiating out to the cell periphery (Fig. 3A). Taxol treatment rearranged MTs from this normal radial array around a single juxtannuclear MTOC into arrays clustered around multiple MTOCs distributed throughout the cytoplasm (Fig. 3B). This effect was seen at doses as low as 100 nM within 15 min of exposure to taxol, although effects were more pronounced at higher doses. This dramatic change in MT and MTOC organization in these cells is quite distinct from the changes seen after treatment with nocodazole.

Taxol Alters Transport of the VSV-G Through the Golgi Apparatus. The Golgi apparatus is localized on MTs near the MTOC and represents a focal point for membrane trafficking within the cell. To test for alterations in the functional

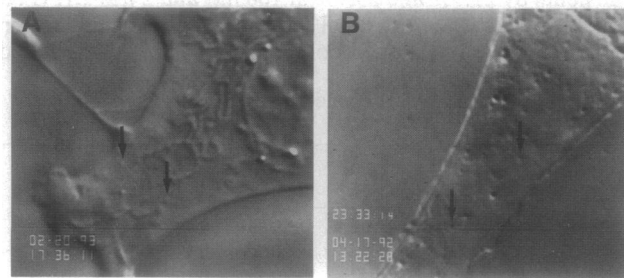


FIG. 1. Video-enhanced DIC microscopy of BAECs. (A) Control. (B) Taxol-treated (4 µM, 60 min, 37°C) BAEC. Arrows indicate vesicles measured in the assay. (×1670.)

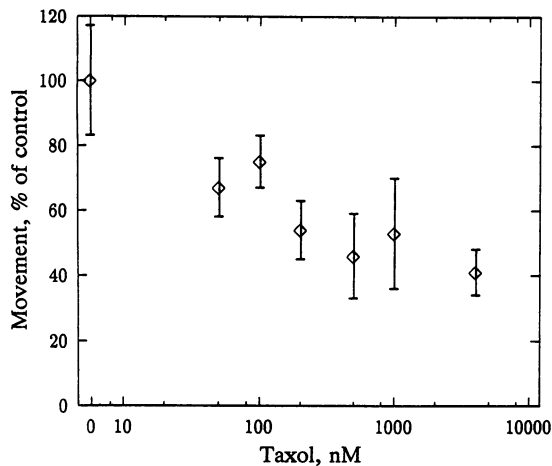


FIG. 2. Dose-response curve for taxol inhibition of frequency of MT-dependent vesicle movements in BAECs. Error bars represent SEMs, and $n \geq 20$ cells for each point.

organization of the Golgi, we followed the transport of a membrane protein, VSV-G, to the Golgi after release from a temperature block. The temperature-sensitive mutant of the virus encoding VSV-G (ts045) allows VSV-G to accumulate in the endoplasmic reticulum at its nonpermissive temperature (39°C). After a shift to the permissive temperature (32°C), VSV-G moves rapidly to the Golgi apparatus. As shown in Fig. 4A, VSV-G in BAECs is found primarily in a juxtanuclear distribution after shift from 39°C to 32°C with the ts045 infection, which is consistent with the transport of this protein to the Golgi. After taxol treatment, however, the released VSV-G is concentrated in two or more sites throughout the cytoplasm (Fig. 4B–D). If VSV-G movement to the Golgi in taxol-treated BAECs is similar to its movement to the Golgi in control BAECs, these data suggest that the Golgi membranes are redistributed in taxol-treated BAECs.

Taxol Effects on the Amplitude of BK- and ATP-Evoked Ca^{2+} Transients. Vasoactive substances such as BK and ATP evoke a Ca^{2+} transient in endothelial cells. The amplitude of the response is proportional to agonist concentration and presumably to density of agonist receptors on the cell surface. Previous work has demonstrated that BK binding to its receptor results in desensitization due to internalization of the BK-BK receptor complex, whereas ATP stimulation does not result in appreciable ATP receptor desensitization (7).

We have measured the intracellular Ca^{2+} transients in BAECs elicited by BK and ATP in control and taxol-treated (4 μ M, 60 min) BAECs. Taxol significantly ($P \leq 0.05$) reduced the peak and decay phase of the BK-evoked Ca^{2+} transient at 2 μ M BK (Fig. 5A *Inset*). The BK dose-peak Ca^{2+} response relationship revealed that taxol significantly ($P \leq 0.05$) reduced the peak value of the BK-evoked Ca^{2+} transients by 21.9% and 23.7% at 100 nM and 2 μ M BK (Fig. 5A). In contrast, 4 μ M taxol had no significant effects on either the early or delayed components of the ATP-evoked

Table 1. Velocity of MT-dependent vesicle movements in taxol-treated BAECs

Taxol, nM	Velocity, μ m/sec
0 (control)	1.50 \pm 0.08
4000	0.83 \pm 0.07*
500	0.96 \pm 0.08*
200	1.04 \pm 0.16*
100	1.40 \pm 0.16

*Significantly different from the control at $P < 0.05$.

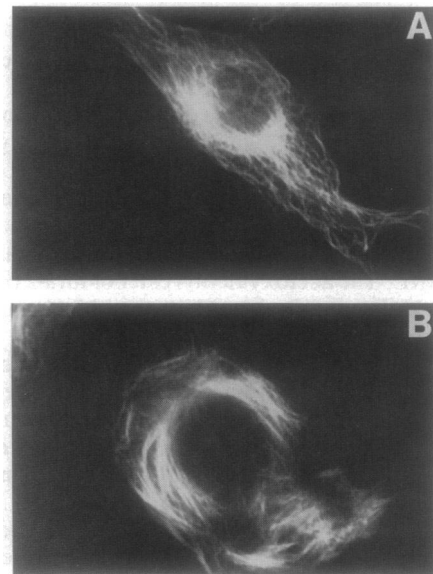


FIG. 3. Tubulin immunofluorescence in BAECs. (A) Control. (B) Taxol-treated (4 μ M, 60 min, 37°C) BAEC.

Ca^{2+} transients or on the ATP dose-peak Ca^{2+} response relationship (Fig. 5B). BK does not alter MT distribution in control or taxol-treated cells (data not shown).

Our data demonstrate that a threshold BK concentration had to be exceeded to elicit taxol's depressant effect on the Ca^{2+} transient, suggesting that receptor saturation during the brief exposure to BK was necessary to detect taxol's effect. As taxol had no significant effect on the ATP response, the effect of taxol on the BK response may be due to receptor desensitization through changes in the recycling pathway.

Desensitization Experiments Show That Taxol Depresses BK-Evoked Ca^{2+} Transients. Since the BK receptor undergoes recycling through a late endosomal or Golgi compartment after BK binding, successive exposures to BK would be expected to result in BK receptor desensitization and reduction in amplitude of the second BK-evoked Ca^{2+} transient relative to that of the first. Recovery from BK desensitization should then be related to the amount of receptor recycled to the surface. To investigate taxol's effects on the recycling of the BK receptor, desensitization experiments were performed in control and taxol-treated BAECs sequentially exposed to two doses of BK or ATP (at 20-min intervals) using measures of $[Ca^{2+}]_i$ to quantitate the degree of receptor

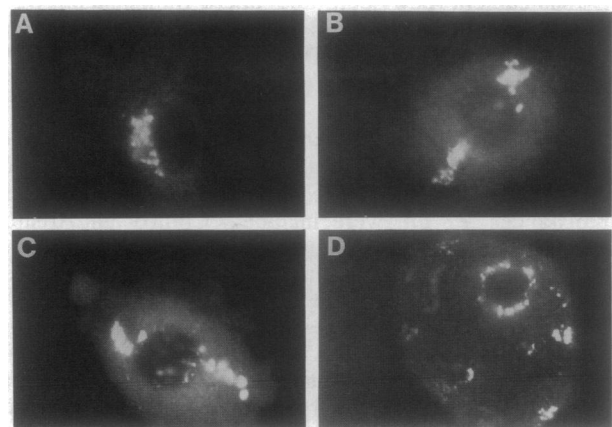


FIG. 4. Immunofluorescence of VSV-G in BAECs infected with ts045 in the absence (A) or presence (B–D) of 4 μ M taxol. Cells were fixed 15 min after release of the temperature block in transport. Taxol (4 μ M) treatment was 60 min at 37°C prior to ts045 infection.

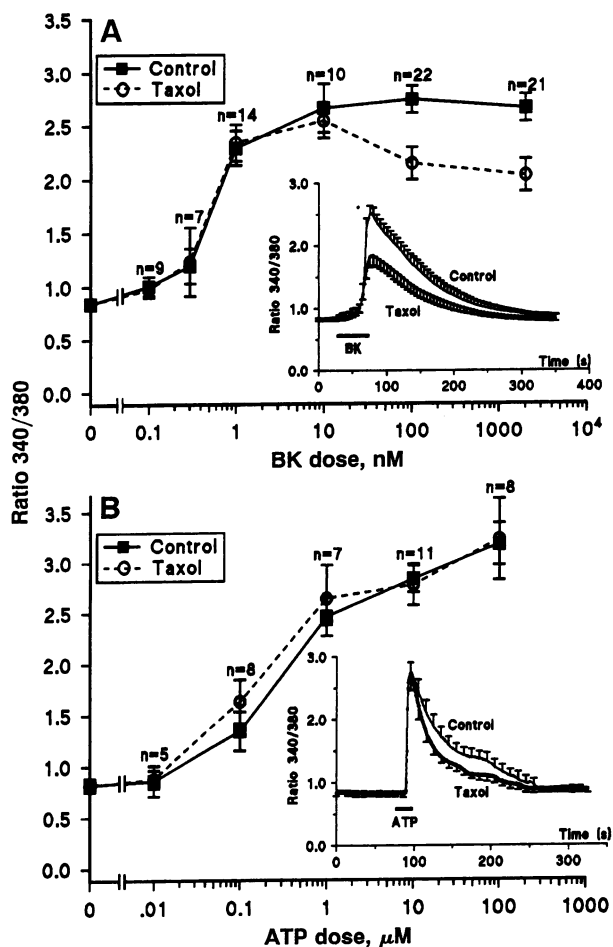


FIG. 5. (A) BK dose-response curve for control and taxol-treated BAECs. (Inset) $[Ca^{2+}]_i$ transients induced by $2 \mu M$ BK (30- to 60-sec exposure) in control and taxol-treated (60 min prior to agonist exposure, $4 \mu M$, $37^\circ C$) BAECs. (B) ATP dose-response curve for control and taxol-treated BAECs. (Inset) $[Ca^{2+}]_i$ transients induced by $10 \mu M$ ATP in control and taxol-treated BAECs. Horizontal bars indicate the presence of agonist during fluorescence measurements.

recycling. Fig. 6 demonstrates that the second BK-evoked Ca^{2+} transient in taxol-treated cells is only $35\% \pm 8.8\%$ ($n = 8$) of the first BK-evoked response (Fig. 6B); in contrast, the second BK-evoked Ca^{2+} transient in control cells is $70.1\% \pm 7.7\%$ of the first BK-evoked Ca^{2+} transient (Fig. 6A). When the same experimental protocol was performed with ATP, the second Ca^{2+} transient elicited by ATP was minimally reduced (Fig. 6C), and taxol had no effect (Fig. 6D). The second ATP-evoked Ca^{2+} transient is $91.7\% \pm 4.5\%$ of the first (Fig. 6D) in taxol-treated cells compared to $91.4\% \pm 3.7\%$ ($n = 10$) in control cells (Fig. 6C).

DISCUSSION

We demonstrate a significant correlation between the taxol-induced decrease in parameters of MT-dependent vesicle transport and the taxol-induced decrease in agonist-evoked Ca^{2+} transients. Since the effects of taxol on agonist-evoked Ca^{2+} transients are specific for BK, whereas ATP-evoked Ca^{2+} transients remained unaffected, the decrease in BK-evoked Ca^{2+} transients correlates with receptor recycling. Cellular organization is altered by taxol, with redistribution of MTs from the normal radial array around the MTOC to multiple MT bundles dispersed in the periphery and alterations in VSV-G processing through the Golgi. We suggest that the taxol-induced alteration in MT structure and orga-

nization generates a change in cell polarity and in this way produces the change in MT-dependent vesicle transport and, consequently, the change in BK receptor recycling. This report on the ability of taxol to alter plasma membrane composition through changes in receptor recycling is important in understanding both the mechanism underlying MT-dependent membrane recycling and a mechanism underlying taxol's cardiovascular toxicity.

For both BK- and ATP-dependent Ca^{2+} transients, the hormonally evoked Ca^{2+} transient is composed of Ca^{2+} both from internal stores and from an influx of Ca^{2+} across the plasma membrane (13, 14). Influx of Ca^{2+} through the plasmalemma appears to occur via a nonselective cation channel, whose activation is dependent on receptor occupancy instead of voltage (15, 16). The effects of taxol on the BK-evoked transient were seen only at concentrations at or exceeding 100 nM . However, sequential exposure to two doses of BK resulted in a more pronounced reduction in amplitude of the second Ca^{2+} transient. Since this effect was negligible with ATP, we interpret the effects of taxol on the BK response to represent a selective decrease in the plasma membrane composition of BK receptors due to changes in receptor internalization (desensitization) and recycling. These effects in turn could impact on vasodilator function of the endothelium by decreasing endothelial release of vasoactive substances such as NO and prostacyclin which are closely coupled to increases in cytosolic Ca^{2+} levels (17-19). Endothelial-mediated relaxation of vascular smooth muscle tone is mediated by endothelial cell response to a variety of vasoactive agents, including BK and ATP. Arachidonic acid release is in part dependent on Ca^{2+} activation of phospholipase A_2 (20). It is clear that the release of vasodilators by endothelial cells is highly dependent upon the integrity of the hormone receptor systems, cell signaling pathways, and membrane ion channels in the plasmalemma and in the endoplasmic reticulum.

Most internal calcium is stored in the endoplasmic reticulum, an organelle with morphology highly dependent on cellular MTs (4, 5). It is possible that alterations in MT structure by taxol could change organization of the endoplasmic reticulum and indirectly perturb Ca^{2+} release. The ability of ATP to elicit the agonist-evoked Ca^{2+} transients in both control and taxol-treated cells is evidence that taxol does not directly affect internal mechanisms of Ca^{2+} release. In addition, we stained cells with 3,3'-dihexyloxycarbocyanine, a fluorescent marker for the endoplasmic reticulum (21), and saw comparable regions of endoplasmic reticulum extended through the periphery of control and taxol-treated BAECs (data not shown). Thus, our data imply that taxol alters membrane receptor composition by its effects on BK receptor desensitization without affecting the Ca^{2+} signaling pathway activated by BK receptor activation.

Nocodazole has previously been reported to alter parameters of MT-dependent vesicle movements (6, 22) and to redistribute the Golgi apparatus (23). In addition, nocodazole apparently causes changes in rates of protein secretion (24) and in protein transport from early to late endosomes (25, 26). However, nocodazole does not alter the recycling of heparin sulfate proteoglycans (27) and the transferrin receptor (27-29) from endosomal compartments and the Golgi to the plasma membrane or the recycling of lipids (30) to the plasma membrane. Although both nocodazole and taxol inhibit vesicle transport, only taxol causes a complete reorganization of MTs that is consistent with a possible change in cell polarity due to redistribution of MT (-) and (+) ends. We believe that the taxol-induced changes in recycling of the BK receptor described here are due to changes in vesicle transport that are elicited through changes in polarity of cellular MTs. Changes in receptor recycling in the endothelium of taxol-treated patients are possibly linked to the development of cardio-

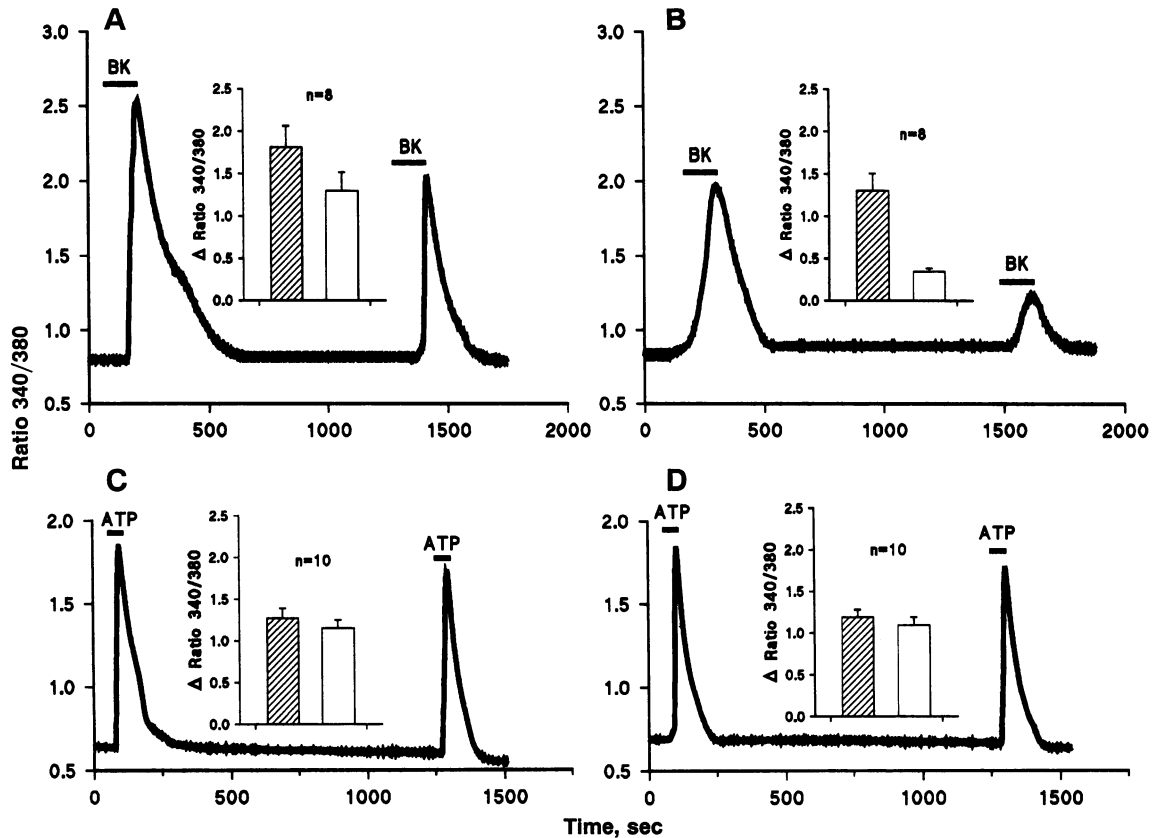


FIG. 6. BK- and ATP-induced changes in $[Ca^{2+}]_i$ in BAECs following repeated stimulation with agonist. (A) $[Ca^{2+}]_i$ transients elicited by 100 nM BK ($n = 8$). (B) $[Ca^{2+}]_i$ transients elicited by 100 nM BK in cells previously treated with 4 μ M taxol for 60 min at 37°C ($n = 8$). (C) $[Ca^{2+}]_i$ transients elicited by 10 μ M ATP. (D) $[Ca^{2+}]_i$ transients elicited by 10 μ M ATP in cells previously treated with 4 μ M taxol for 60 min at 37°C. (Inset) Summary of peak ratios for $[Ca^{2+}]_i$ transients elicited by agonist desensitization experiments in BAECs with (B, D) and without (A, C) taxol. Hatched bar, initial agonist exposure; open bar, second agonist exposure. Exposure to BK or ATP (30–60 sec) was followed by rinsing with a BK- or ATP-free physiological solution for 20 min. Cells were then reexposed to the agonist (30–60 sec) and washed with an agonist-free physiological solution. Horizontal bars indicate the presence of an agonist. Taxol treatment (4 μ M, 60 min, 37°C) was prior to the first agonist exposure, and all subsequent perfusions for the taxol-treated cells also contained 4 μ M taxol. Ratio 340/380 values were measured from the resting ratio to ratio at the transient peak caused by application of agonist.

vascular toxicity. The failure of colchicine and the vinca alkaloids to elicit cardiovascular toxicity comparable to that of taxol is expected because these drugs do not cause comparable changes in cell polarity. The availability of new taxol analogs such as taxotere will provide us with additional tools for understanding the mechanism underlying taxol's effects on MT-dependent membrane recycling.

We thank Jim McIlvain for assistance with VSV-G experiments and R. Michael Alvarez for assistance with statistical analysis. S.F.H.-A. was supported by a postdoctoral fellowship from the Muscular Dystrophy Association and aided by Grant IRG-21-33 from the American Cancer Society. M.P.S. was supported by National Institutes of Health (NIH) Grants GM 36277 and NS 23345. H.C.S. was supported by NIH Grants HL 45132, 19216, and 17670.

- Wani, M. C., Taylor, H. L., Wall, M. E., Doggon, P. & McPhail, A. T. (1971) *J. Am. Chem. Soc.* **93**, 2325–2327.
- Rowinsky, E. K., Eisenhauer, E. A., Chaudhry, V., Arbuck, S. G. & Donehower, R. C. (1993) *Semin. Oncol.* **20**, 1–15.
- Schiff, P. B., Tant, J. & Horwitz, S. B. (1979) *Nature (London)* **22**, 665–667.
- Schroer, T. A. & Sheetz, M. P. (1991) *Annu. Rev. Physiol.* **53**, 629–652.
- Skoufias, D. A. & Scholey, J. M. (1993) *Curr. Opin. Cell Biol.* **5**, 95–104.
- Hamm-Alvarez, S. F., Kim, P. Y. & Sheetz, M. P. (1993) *J. Cell Sci.* **106**, 955–966.
- Weintraub, W. H., Negulescu, P. A. & Machen, T. E. (1992) *Am. J. Physiol.* **263**, C1029–C1039.
- Munoz, C. M. & Leeb-Lundberg, L. M. F. (1992) *J. Biol. Chem.* **267**, 303–309.
- Jaffe, E. A., Nachman, R. L., Becker, C. G. & Minick, C. R. (1973) *J. Clin. Invest.* **52**, 2745–2756.
- Toyoshima, I., Yu, H. & Sheetz, M. P. (1992) *J. Cell Biol.* **118**, 1121–1131.
- Kreis, T. E. (1986) *EMBO J.* **5**, 931–941.
- Schnapp, B. J. (1986) *Methods Enzymol.* **134**, 561–573.
- Schilling, W. P., Rajan, L. & Strobl-Jager, E. (1989) *J. Biol. Chem.* **264**, 12838–12848.
- Dolor, R. J., Hurwitz, L. M., Mirza, A., Strauss, H. C. & Whorton, A. R. (1992) *Am. J. Physiol.* **262**, C171–C181.
- Luckhoff, A. & Clapham, D. E. (1992) *Nature (London)* **355**, 356–358.
- Nilius, B. (1990) *Pflügers Arch.* **416**, 609–611.
- de Nucci, G., Gryglewski, R. J., Warner, T. D. & Vane, J. R. (1988) *Proc. Natl. Acad. Sci. USA* **85**, 2334–2338.
- Jaffe, E. A., Grulich, J., Weksler, B. B., Hampel, G. & Watanabe, K. (1987) *J. Biol. Chem.* **262**, 8557–8565.
- Carter, T. K., Hallam, T. J., Cusack, N. J. & Pearson, J. D. (1988) *Br. J. Pharmacol.* **95**, 1181–1190.
- Buckley, B. J., Barchowsky, A., Dolor, R. J. & Whorton, A. R. (1991) *Biochem. J.* **280**, 281–287.
- Lee, C. & Chen, L. B. (1988) *Cell* **54**, 37–46.
- De Brabander, M., Nuydens, R., Geerts, H. & Hopkins, C. R. (1988) *Cell Motil. Cytoskel.* **9**, 30–47.
- Thyberg, J. & Moskalewski, S. (1985) *Exp. Cell Res.* **159**, 1–16.
- Tooze, S. A., Flatmark, T., Tooze, J. & Huttner, W. B. (1991) *J. Cell Biol.* **115**, 1491–1503.
- Diaz, R., Columbo, M. I., Koval, M., Mayorga, L. & Stahl, P. (1991) *Eur. J. Cell Biol.* **56**, 223–232.
- Gruenberg, J., Griffiths, G. & Howell, K. E. (1989) *J. Cell Biol.* **108**, 1301–1316.
- Takeuchi, Y., Yanagashita, M. & Hascall, V. C. (1992) *J. Biol. Chem.* **267**, 14685–14690.
- Jin, M. & Snider, M. D. (1993) *J. Biol. Chem.* **268**, 18390–18397.
- Sakai, R., Yamashina, S. & Ohnishi, S. (1991) *J. Biochem.* **109**, 528–533.
- Koval, M. & Pagano, R. E. (1989) *J. Cell Biol.* **108**, 2169–2181.